Power Loss and Thermal Characterization of IGBT Modules in the Alternate Arm Converter

P. D. Judge, M. M. C. Merlin, P. D. Mitcheson, T. C. Green
Control and Power Group, Department of Electrical and Electronic Engineering, Imperial College London
p.judge12@imperial.ac.uk, michael.merlin07@imperial.ac.uk, p.mitcheson@imperial.ac.uk, t.green@imperial.ac.uk

***Abstract*—Power losses in high power HVDC converters are dominated by those that occur within the power electronic devices. This power loss is dissipated as heat at the junction of semiconductor devices. The cooling system ensures that the generated heat is evacuated outside the converter station but temperature management remains critical for the lifetime of the semiconductor devices. This paper presents the results of a study on the temperature profile of the different switches inside a multilevel converter. The steady state junction temperatures are observed through the simulation of a 20 MW Alternate Arm Converter using 1.2kA 3.3 kV IGBT modules. A comparison of the Alternate Arm Converter is made against the case of both the half-bridge and full-bridge Modular Multilevel Converter topologies. Furthermore, the concept of varying the duty-cycle of the two alternative zero-voltage states of the H-bridge modules is introduced. Simulation results demonstrate that it can change the balance of electrical and thermal stress between the two top switches and the two bottom switches of a full-bridge cell.**

I. Thermal Design Considerations and Importance

Manufacturers typically require that the maximum junction temperature of IGBT modules is limited to below 150°C, or 125°C, and that the operating temperature under normal conditions be limited to 80% that of the maximum value [1], [2]. Devices with higher current ratings are typically limited to the lower value of 125°C. Operating the device above this level can lead to a breakdown in reverse voltage blocking capability and thermal runaway, leading to device destruction. The system must be designed so that the junction temperature (T_j) never exceeds this value. The level of power and thermal cycling that a module undergoes during its operation can have a large impact on the expected lifetime of the module. Power cycling, which occurs at time frames of around 2 seconds causes stress in the soldering of the electrical connections within the IGBT module due to the different coefficients of linear expansion. If the power cycling causes the soldering to deteriorate sufficiently then the device will experience electrical failure. At a longer time frame and with a larger change in temperature ($\triangle T_j$), thermal cycling of IGBT modules causes unequal expansion of the insulation substrate and the copper base-plate and fatigue to the solder layer between them [1]. This can lead to device failure as it causes the thermal resistance of the module to increase, leading to thermal runaway. Manufacturers usually supply power cycle and thermal cycle capability curves for IGBT modules which allow the estimation of the lifetime of the modules. The degradation of lifetime is dependent on absolute junction temperature as well as the magnitude of the power or thermal cycle [3]. Looking beyond lifetime issues for high power applications, it is desirable to keep the junction temperature as low as reasonably possible. This is because the level of thermally generated electron hole pairs increases with temperature, thus decreasing the devices conductivity and ultimately leading to an increase in power loss.

The authors gratefully acknowledge the financial support of the Research Councils UK through the HubNet Project (grant number: EP/I013636/1)

II. Power Loss Modeling

A Matlab/Simulink block was created to estimate the power losses within each IGBT module within a converter following the technique presented in [4]. This method uses the current flowing through each module as well as the gate signal to detect switching events to determine the expected losses. The waveforms in the simulated converter are assumed to not be impaired by the on-state resistances of switching elements within Matlab/Simulink as the overall losses are small. This Simulink block outputs the power losses occurring at the IGBT junction and the diode junction within a module, which can then be applied to a thermal model of the device to determine the expected junction temperatures. This method is suitable for use within fixed-step discrete real-time simulations and calculates the power loss at each time step within the simulation. This method has been verified against the results of a post-processing script method used in [5]. The loss curves needed for this method were extracted from the manufacturers datasheet and where possible scaled for an operating temperature of 75°C.

III. Thermal Modeling

The thermal model of the IGBT used within this study was developed using the Finite Element Method (FEM) electronics thermal simulation package ANSYS IcePak. The Device used is a 1.2kA 3.3kV 5SNA 1200E330100 module from ABB Semiconductors [6]. The module modeled within ANSYS IcePak is shown in Figure 1.

The thermal modeling of a similar heat sink mounted IGBT module and validation against experimental results has been extensively covered in [7]. The thermal model within this study

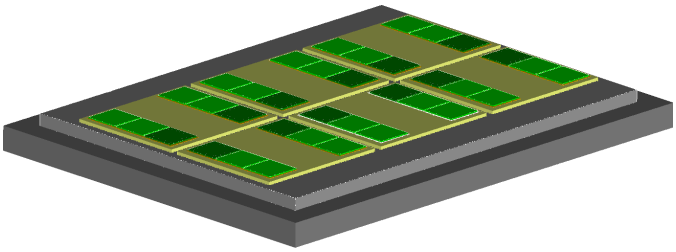

Figure 1: Heat-sink mounted IGBT modeled within ANSYS IcePak

has been compared against the results presented in [7], and agrees with close approximation.

The internal construction and thermal design of the device is detailed in [2]. Internally the device consists of 24 IGBT dies and 12 diode dies connected by internal bus bars and bond wires. The diode dies are located closest to the center of the device. In the model it is assumed that all heat flow is from the active junctions to the cooling liquid of the heat-plate and that any heat flow from the junction to ambient air is negligible, for this reason the plastic case, bond wires and internal bus bars of the module are not included in the model. The power losses are modeled as 2-D power sources, dissipating a fixed amount of power, placed upon the top surface of each die. The dies within the module are assumed to equally share the overall power loss within the module due to the positive temperature coefficient of the on-state voltages of each die.

The junction temperatures are measured at the geometric center of each silicon die. Due to the internal construction of the device there is a varying amount of cross coupling between the dies which leads to an imbalance between junction temperatures of individual dies within the module. The junction temperature measurements presented in this study are an average of the junction temperatures measured at each IGBT or diode die within the module. The thermal model has also been verified against the transient thermal impedance curves provided by the manufacturer in the data-sheet by using a 2-D temperature source to hold the external case temperature to a fixed value. In real applications, holding the case temperature at a constant temperature is not practical so it is necessary to model the heat sink on which the module is mounted. The heat sink also acts as a heat spreader, increasing the level of cross coupling between the dies within the module [7].

$$Z_{th}(t) = \sum \gamma_i.(1 - exp(\frac{-t}{\tau_i})) \qquad (1)$$

The transient thermal impedance response curves of the module to both sets of dies being heated are shown in Figure 2. To derive thermal models suitable for use within the Matlab/Simulink model the transient thermal impedance curves are fitted to a finite series of exponential terms in the form of (1). The Laplace transform is then applied to this finite series to give a transfer function suitable for use in a Matlab/Simulink simulation of the converter.

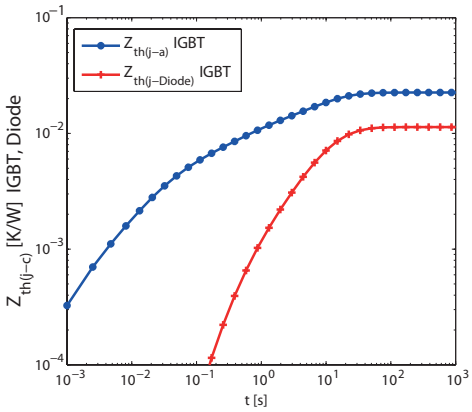

(a) IGBT dies heated

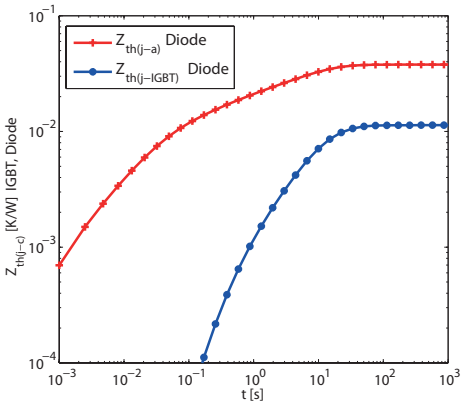

(b) Diode dies heated

Figure 2: Transient thermal impedance response

IV. Modular Multi-Level Converters and the Alternate Arm Converter

The primary focus of this paper is the thermal characterization of the IGBT modules within the Alternate Arm Converter (AAC), which was introduced in [5] and is illustrated in Figure 3. However for comparison purposes an analysis of half-bridge Modular Multilevel Converter (MMC), illustrated in Figure 4, and the full-bridge MMC is also presented. Functionally the full-bridge MMC and standard half-bridge MMC have similar operation though the full-bridge MMC adds the potential to block DC side faults due to its ability to control the converters inductor currents during a fault. This ability comes at a cost of needing twice as many semiconductor switches and a doubling of the conduction losses within the converter.

The AAC is a hybrid topology between the 2-level converter and the MMC first introduced in [8]. As with the

MMC, the AAC utilizes stacks of H-bridge cells (in their 4-switch version, shown in Figure 3) in its arms but with director switches to alternate the working of the arms leading to several key features distinct from the MMC. Firstly, this mode of operation rectifies the AC current directly instead of requiring an additional DC current running continuously through the

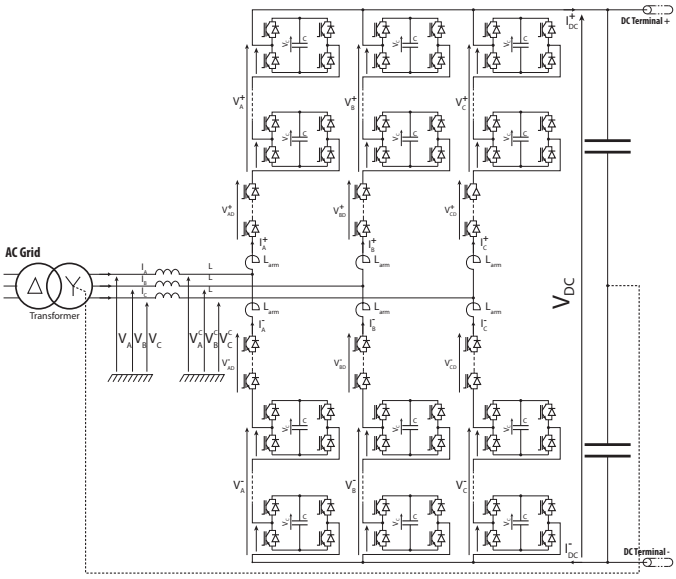

Figure 3: Alternate Arm Converter

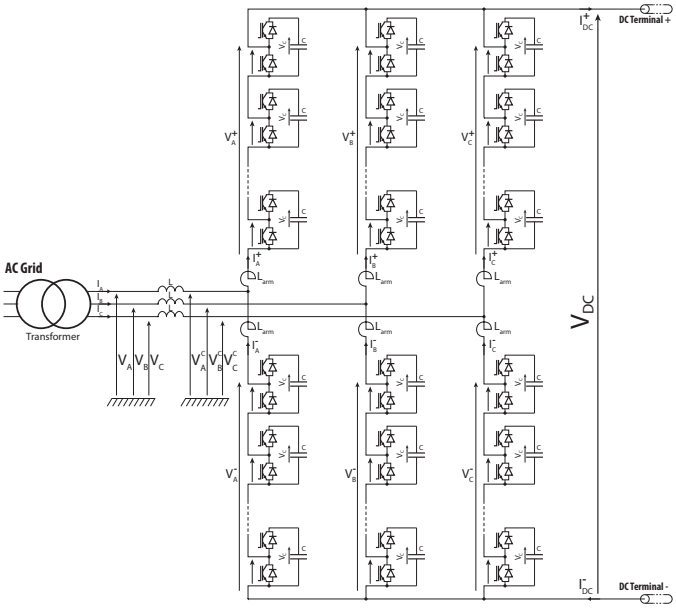

Figure 4: Half-bridge Modular Multi-Level Converter

arms. Secondly, the number of cells in the stacks is much reduced because each arm is used to produce only half of the converter AC voltage waveform. Thirdly, the AAC is able to block DC-side fault currents passing through its arms because full-bridge cells can produce negative voltage to oppose the AC grid voltage, and hence keep control of the stack. Finally, the director switches can be operated in soft-switching mode, i.e. switching off when their current reaches zero, thanks to the arm currents being kept under tight control by the stacks.

A comparison of the arm currents and voltages within the AAC and the MMC is shown in Figure 5. The primary difference between the two is that each arm of the AAC conducts current for half of each electrical cycle and can generate

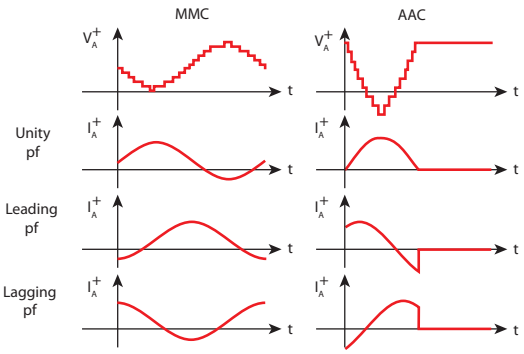

Figure 5: AAC and MMC top arm current and voltage

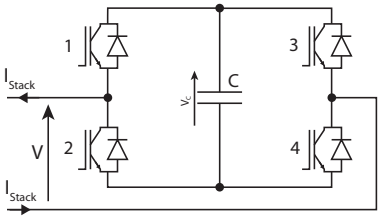

(a) Full-bridge cell

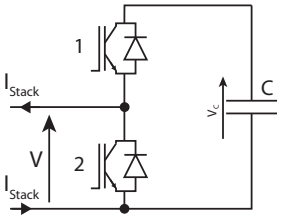

(b) Half-bridge cell

Figure 6: Full-bridge and half-bridge cell configurations

a negative DC voltage which allows an over-modulated AC voltage, greater than the DC voltage. In comparison each cell within an MMC conducts current for the entire electrical cycle and is unable to generate a negative voltage.

V. Full-Bridge and Half-Bridge Configurations

Both the AAC and the full-bridge MMC make use of a full-bridge cells rather than a half-bridge cells as used in the standard MMC topology. Both cell arrangements are shown in Figure 6, with voltage and current definitions given using a source convention.

A full-bridge has effectively four states with three different voltage outputs. The AAC utilizes all three possible voltage outputs whilst the full-bridge MMC is limited to using the positive voltage output and the two zero voltage output states during normal operation. The path that the arm current takes through the cell depends on current direction and cell voltage output (or state). For a full-bridge cell this path is always through two separate modules. The path that the current takes is shown in Table I. A half-bridge has two states with two possible voltage outputs. The current paths for these states are shown in Table II.

Table I: Current path through a full-bridge cell depending on stack current direction and cell voltage output

(a) I_{stack} Positive

	IGBT Position			
V_{out}	**1**	**2**	**3**	**4**
$+V_{cell}$	IGBT			IGBT
0	IGBT		Diode	
0		Diode		IGBT
$-V_{cell}$		Diode	Diode	

(b) I_{stack} Negative

	IGBT Position			
V_{out}	**1**	**2**	**3**	**4**
$+V_{cell}$	Diode			Diode
0	Diode		IGBT	
0		IGBT		Diode
$-V_{cell}$		IGBT	IGBT	

Table II: Current path through a half-bridge cell depending on stack current direction and cell voltage output

(a) I_{stack} Positive

	IGBT Position	
V_{out}	**1**	**2**
$+V_{cell}$	IGBT	
0		Diode

(b) I_{stack} Negative

	IGBT Position	
V_{out}	**1**	**2**
$+V_{cell}$	Diode	
0		IGBT

For converter with full-bridge cells, the zero-voltage state duty cycle (δ_{zv}) of each cell has been defined as the ratio of how often the combination of IGBTs 2 and 4 is selected, as opposed to the combination of IGBTs 1 and 3, to how often either zero-voltage state is used. A δ_{zv} of 0% corresponds to only IGBTs 1 and 3 being selected for zero voltage generation and a δ_{zv} of 100% corresponds to only IGBTs 2 and 4 being selected for zero voltage generation. Unless specified otherwise, a δ_{zv} of 50% has been used in the simulations, meaning that a random distribution between the two possible states is used.

VI. Power Loss and Thermal Characterization

The power losses within each module of a single cell were determined by simulation and are plotted for different operating points of the three converter topologies under examination. Each point is an average power loss over 3 s of steady-state operation so as to avoid any short-term effects arising from the control system. The power flow convention used is that negative power is AC power being rectified to DC and positive power is DC power being inverted to AC. The cooling water temperature for all results shown is assumed to be 40°C.

A. The Alternate Arm Converter

The power losses and junction temperatures as a function of real power for each IGBT module of a single cell within an AAC in addition to one IGBT forming part of the director switch in the same arm are shown in Figure 7.

As is shown in Figure 7, the power losses within each IGBT module occur almost exclusively within either the IGBT or the diode, depending on whether the converter is in rectifying or inverting mode and varying with real power flow. This is because, at unity power factor, the current flowing through each arm of the AAC is either nominally continually positive or continually negative. The director switch exhibits higher power losses, leading to a higher junction temperature than any of the switches in the cells in spite of having close to zero switching losses. This can be explained by the fact that the director switches are in conduction for the whole working period of their arm while the switches in the cells are periodically switched out of the conduction path, in addition conduction losses dominate switching losses in MMC derivative converters.

The results indicate that the losses within each cell should be approximately equal regardless of the power flow direction. However the power losses and junction temperatures reached within the director switch modules will be higher during inverting operation due to the higher on state voltage drop of the IGBT in comparison to the diode.

The results indicate that the AAC will operate with a maximum junction temperature that is significantly below the maximum permissible value of 125°C (given the 40°C ambient coolant temperature). In the director switches, there is 63°C of headroom to 125°C for the IGBTs and 59°C for the diode. In the cells, there is 69°C of headroom to 125°C for the IGBTs and 68°C for the diodes. Furthermore, the results show that there is a good distribution of electrical and thermal stress between each of the IGBT modules within the cell when δ_{zv} is set to 50%. The B_{10} lifetime curves, provided by the manufacturer in [3], indicate that that thermal and power cycling impacts on lifetime should not be significant, even when extreme cases such as regular power flow reversals are considered.

B. The Half-Bridge Modular Multi-Level Converter

The power losses and junction temperatures within each IGBT module of a single cell within a half-bridge MMC are shown in Figure 8.

As shown in Figure 8, there is a large imbalance between the power losses generated within the two modules, with most of the losses occurring in IGBT 2. Additionally In IGBT 1 the power losses are split almost equally between the IGBT and the diode whereas in IGBT 2 the power losses occur almost exclusively in either the IGBT or diode, depending on power flow direction. This can be explained by examining the voltage waveforms shown in Figure 5. When the stacks are generating a low voltage, i.e. most of the cells within an arm are bypassed using IGBT 2 within each cell, the current flowing though the arm approaches its highest level resulting in high losses in either the diode or IGBT within this module . During the rest of the cycle when the stack is generating an intermediate or high voltage, i.e. when the cells are more likely to be to be generating an output of $+V_{CELL}$, the current is lower in magnitude and for part of the cycle reversed in direction, changing the nominal current path through the module which

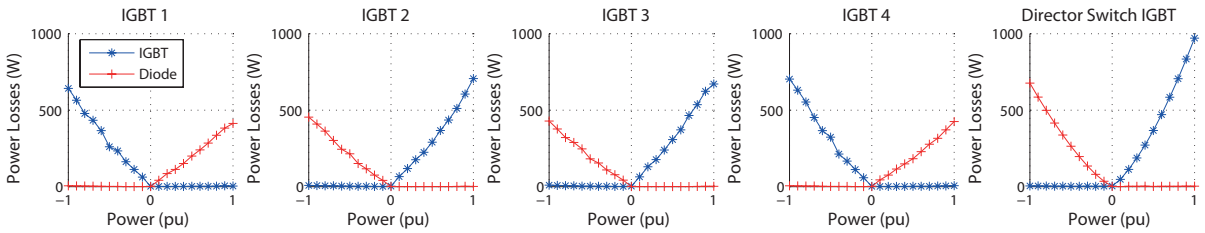

(a) Power Losses

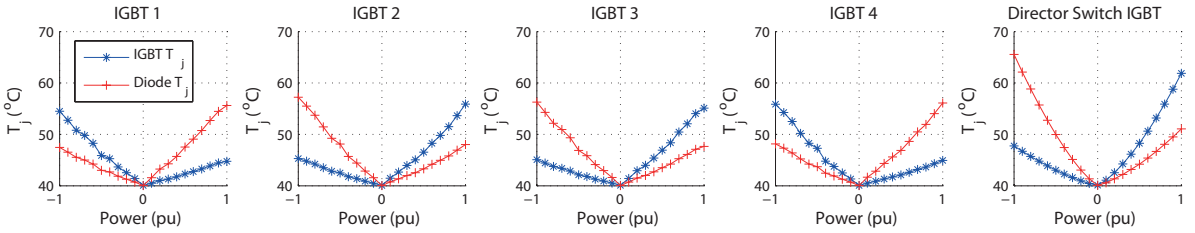

(b) Junction Temperatures

Figure 7: Power Loss and junction temperatures of modules within the AAC at unity power factor

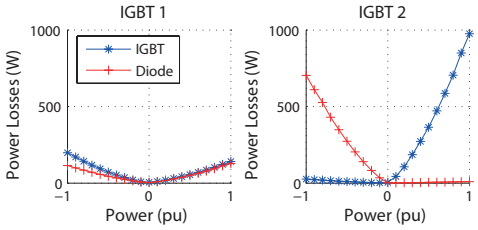

(a) Power Losses

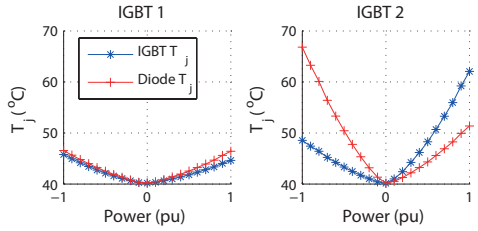

(b) Junction Temperatures

Figure 8: Power Loss and junction temperatures of modules within the half-bridge MMC at unity power factor

results in the split of losses between IGBT and diode observed in module 1.

Similar to the AAC director switch, the results indicate that the losses within each cell will be higher during inverting operation. The results also indicate that the maximum junction temperatures reached within the half-bridge MMC are similar to those reached by the director switch module within the AAC, but lower than the temperatures reached within the cells of the AAC.

C. The Full-Bridge Modular Multi-Level Converter

The power losses and junction temperatures within each IGBT module of a single cell within an full-bridge MMC are shown in Figure9.

Similar to the half-bridge MMC, the power losses are split between the IGBT and the diode within each IGBT module. IGBTs 1 and 4 experience larger losses than IGBTs 2 and 3. This can be explained by examining the current path through each cell shown in Table I. IGBTs 1 and 4 each form part of the current carrying path for two possible states, during the positive voltage output state, and each during one of the two possible zero voltage output states. As the negative voltage output state of the cell is unused in the full-bridge MMC topology, IGBTS 2 and 3 each only form part of the current carrying path during one of the two possible zero voltage output states. As IGBTs 2 and 3 are utilized less than IGBTs 1 and 4 they experience lower losses.

In contrast the half-bridge MMC cell and the director switch of the AAC the power losses within appear to be greater during rectifying operation. Given the maximum junction temperature reached, there is 62°C of headroom to 125°C.

VII. Impact of Duty-Cycle of Zero-Voltage States

As discussed in the introduction, by varying the duty-cycle of the zero-voltage states (δ_{zv}), the electrical and thermal stress within each cell can be redistributed. This can be used to more evenly spread the thermal and electrical stress between switches. The extent to which this method is effective for the AAC operating at rated power is illustrated in Figure 10.

In both rectifying and inverting operation the optimal duty cycle for balancing the losses between the IGBT modules within a cell appears to be close 50%. The results indicate that by varying the value of δ_{zv}, the electrical load upon individual IGBT switches can be varied by up to approximately 800 W. This represents a percentage change in power losses of approximately 57% above or below the nominal power losses when δ_{zv} is set to 50%. Correspondingly the junction temperature of individual devices can be varied over a range of approximately 20°C. This method has a limitation in that the

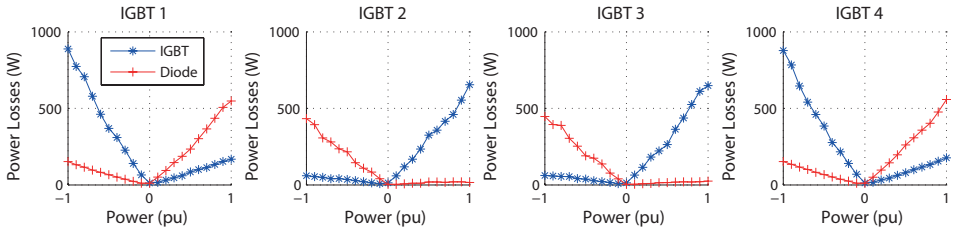

(a) Power Losses

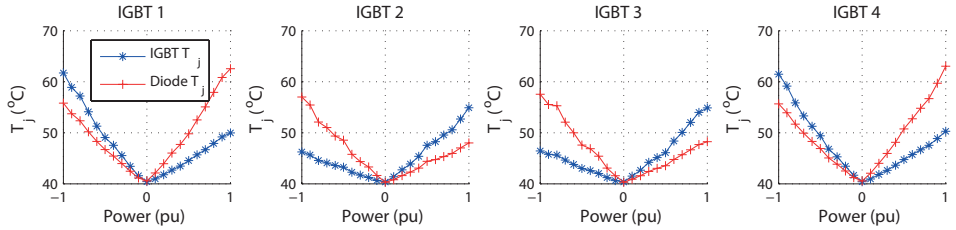

(b) Junction Temperatures

Figure 9: Power loss and junction temperatures of the full-bridge MMC at unity power factor

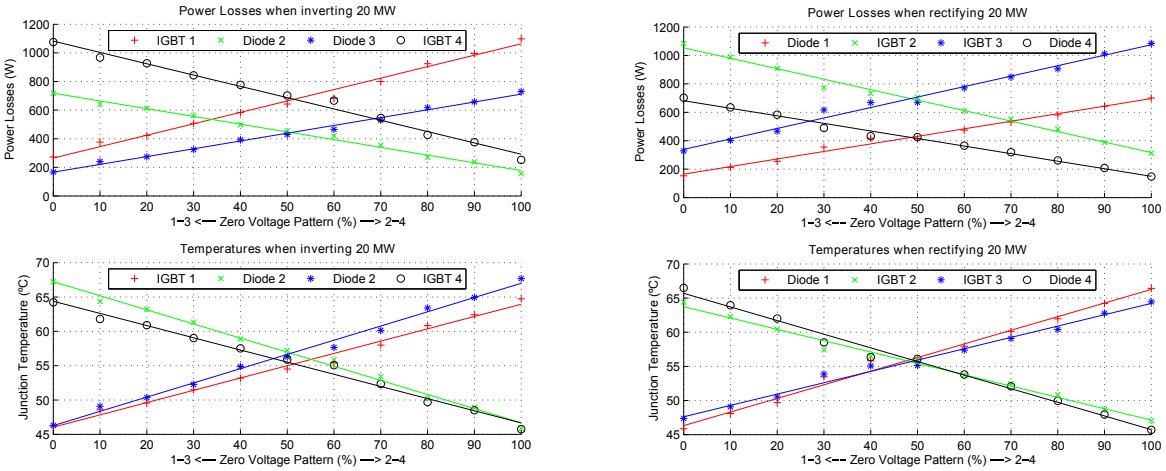

(a) Inverting operation

(b) Rectifying operation

Figure 10: Power losses and temperatures of modules within an AAC for different values of δ_{zv} at rated power

power losses within IGBTs 1 and 3 are coupled and similarly the power losses within IGBTs 2 and 4 are coupled.

VIII. Online thermal management using the zero voltage duty cycle

It has been shown that it is possible to significantly affect which modules within each cell of the AAC experience the most power losses by varying the zero voltage duty cycle.

By using this method with a feedback mechanism, it should be possible to move some of the thermal and electrical stress being placed upon a module which has been detected as deteriorating on to the other healthier modules within the cell. This could be achieved by measuring a temperature dependent characteristic, such as the V_{ce}-I_{ce} relationship or by taking a measurement of the modules case temperature.

Using the ANSYS model of the heat-sink mounted IGBT module the transient thermal impedance from the IGBT and diode junctions to an external point on the base-plate of the module was determined. This point was selected so that the thermal resistance from IGBT junction and the diode junction to the measuring point was approximately equal.

As the thermal stress placed IGBTs 1 and 4 and upon IGBTs 2 and 3 are coupled the proposed control scheme was picked to try drive the difference between the sum of the thermal stress on each coupled pair to zero. The control scheme is shown schematically in Figure 11, where $C(s)$ represents the controller.

The controller used was a simple proportional-integral controller with a low gain, given the slow dynamics, to ensure good steady state regulation. The results of a 250 second

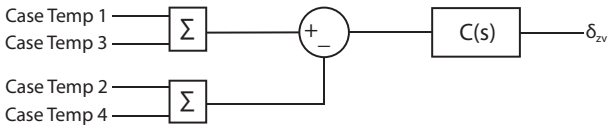

Figure 11: Zero voltage duty cycle feedback control scheme overview

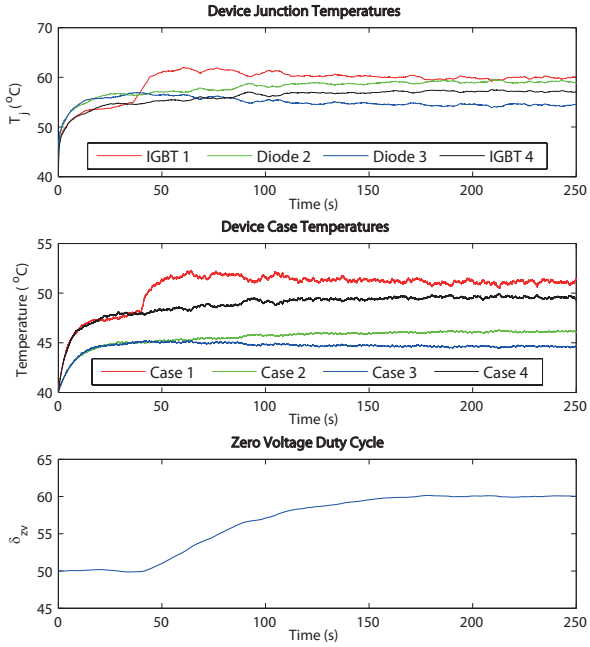

Figure 12: Zero voltage duty cycle feedback demonstration

long simulation are shown in Figure 12. At 40 seconds, the degradation of IGBT module 1 is simulated by increasing the power losses within the module by 50%, resulting in increase in its junction temperatures and the case temperature at the measurement point. This imbalance causes the compensator to adjust the value of δ_{zv}, moving some of the thermal stress away from IGBT modules 1 and 4 and on to IGBT modules 2 and 3. The system has a settling time of approximately 200 seconds before it reaches a steady-state value. The power flow during this simulation remained at a constant 20MW in rectifying mode.

IX. Conclusion

A power loss and thermal study of the semiconductor devices in the AAC and the half-bridge and full-bridge variants of the MMC has been conducted and the results indicate that the devices in all of these converters should be expected to operate well below the maximum allowable junction temperature and allow a significant safety margin. Comparing the AAC to both the half-bridge MMC and full-bridge MMC shows that the maximum junction temperature of devices within the cells of the AAC should be expected to be lower than either of the MMC formats because of lower overall cell power loss. However, the devices in director switches of the AAC suffer relatively high conduction losses and therefore relatively high junction temperature.

The power loss and thermal analysis of these converters has also led to the development of a convenient mechanism for balancing temperature rise of the devices within a cell. It is called the zero-voltage state duty-cycle (δ_{zv}) and it sets how often each of the two possible zero-voltage output states of a full-bridge cell is selected. By varying this duty-cycle, a significant amount of electrical and thermal stresses can be transferred between IGBTs 1 and 3, which form the current carrying path in one state, and IGBTs 2 and 4, which form the current carrying path in the other state. A simple feedback mechanism for controlling this duty-cycle online and thereby balancing the power losses between modules within a cell without disrupting the operation of the converter has also been demonstrated by simulation.

References

[1] Mitsubish Electric Ltd, "IGBT Modules Application Note: The 5th Generation IGBT Chip use," December 2007. [Online]. Available: http://www.mitsubishielectric.com/semiconductors/files/manuals/igbt_note_e.pdf

[2] ABB, "Application Note: Thermal Design and Temperature Ratings of IGBT Modules." [Online]. Available: http://www.abb.com/semiconductors

[3] ABB, "Load-cycling capability of HiPak IGBT Modules." [Online]. Available: {http://www.abb.com/semiconductors}

[4] Z. Luo, "A Thermal Model For Igbt Modules And Its Implementation In A Real Time Simulator," Ph.D. dissertation, University of Pittsburgh, 2002.

[5] M. M. C. Merlin, T. C. Green, P. D. Mitcheson, D. R. Trainer, D. R. Critchley, and R. W. Crookes, "A new hybrid multi-level Voltage-Source Converter with DC fault blocking capability," in *AC and DC Power Transmission, 2010. ACDC. 9th IET International Conference on*, oct. 2010, pp. 1 –5.

[6] ABB HiPak IGBT Module 5SNA 1200E330100. Datasheet available online. [Online]. Available: http://www.abb.com/semiconductors

[7] U. Drofenik, D. Cottet, A. Müsing, J. M. Meyer, and J. W. Kolar, "Modelling the thermal coupling between internal power semiconductor dies of a water-cooled 3300V/1200A HiPak IGBT module," in *Proceedings of Power Conversion and Intelligent Motion Conference*, 2007.

[8] A. Lesnicar and R. Marquardt, "An innovative modular multilevel converter topology suitable for a wide power range," in *Power Tech Conference Proceedings, 2003 IEEE Bologna*, vol. 3, june 2003, p. 6 pp. Vol.3.